Dynamic fracture of advanced ceramics under impact loading conditions using a miniaturized Kolsky bar

Declan McNamara*, Patricia Alveen[1], Declan Carolan[1], Neal Murphy[1], Alojz Ivanković[1]

[1] School of Mechanical and Materials Engineering, University College Dublin, Ireland
* Corresponding author: Declan.mc-namara@ucdconnect.ie

Abstract
Advanced ceramic materials are frequently used in the machining of hardened steels, aerospace alloys and other abrasive materials. While these materials have many superior properties such as high hardness and abrasive resistance they are still prone to premature failure due to fracture. Accurate fracture properties of such materials are scarce, especially in the dynamic regime. The current work presents a novel combined experimental-numerical approach to determine dynamic fracture behavior. In recent years, much attention has been given to the study of dynamic behavior of materials under stress-wave loading. Experimentation with a modified Kolsky bar and a concurrent numerical investigation using the finite volume method was used in this study. The inherent difficulties in producing large amounts of advanced ceramic means that experiments must be carried out using very small samples. As a result the apparatus has been miniaturised to accommodate such specimen dimensions. The incident and reflected wave histories obtained experimentally in conjunction with the time to fracture of the specimen predicted numerically are used to determine fracture toughness at a number of loading rates.
Presented is a novel and simple test method to determine fracture properties of advanced ceramics using a miniaturised Kolsky bar. Results indicate a change in fracture toughness at increased rates of loading. This may be due to the complicated underlying microstructure of the materials under investigation, which behave differently under varying loading rates.

Keywords Dynamic Fracture, miniaturized Kolsky bar, advanced ceramics

1. Introduction

As opposed to static fracture toughness, no standard methodology yet exists for the determination of the dynamic fracture toughness of materials. Under static conditions the stress intensity factor at the crack tip is proportional to the applied load, under dynamic loading this does not hold true. This is due to the inertial effects, which result from the transient loading conditions. Other factors affecting the determination of dynamic fracture toughness include wave propagation within the test specimen and the accurate determination of crack initiation.

Traditionally dynamic fracture experiments were performed using the instrumented Charpy pendulum [1]. In this test setup strain gauges mounted on the hammerhead measure the response resulting from the impact on a specimen, [2, 3]. While this test method is well established and easily performed there exists a number of drawbacks. During the dynamic impact strong inertial forces affect the load applied at the crack tip. The hammer impact load is recorded by the strain gauge located at its head and this is used to determine the fracture parameters through the resulting load-time history. However due to the inertial forces present the applied load recorded by the

hammer head will be significantly different to that experienced at the crack tip. The impact of the hammer on the specimen will generate longitudinal and traverse stress waves within the specimen and these stress waves will influence the stress intensity factor at the crack tip [4]. Experimental results from the Charpy test are therefore difficult to interpret, as large inertial oscillations are often present in the load-time histories.

To overcome the limitations posed by traditional dynamic test methods much attention has recently been given to the study of dynamic behavior of materials under stress wave loading using a modified Kolsky bar, [5, 6, 7]. The Kolsky bar apparatus allows for fracture testing at rates greater the 10^6 MPa$\sqrt{m}$ s^{-1} therefore simulating more realistic loading conditions experienced by super-hard materials during operation. Both the tensile and compressive loading configurations have been adopted for fracture testing. For the most part compressive stress pulse loading has been most popular and following on from the standard quasi-static setup the high rate-bending configuration has proliferated. Detailed descriptions of all Hopkinson bar fracture tests can be found in a review paper by Fengchun *et al*. [8].

Fracture toughness values presented in this paper should be considered to be measured or apparent fracture toughness's, (K_{1db}) as opposed to the critical dynamic fracture toughness, (K_d). This is due to the effect of notch tip blunting in dynamic fracture tests and the effect of finite notch root radii on the overestimation of the fracture toughness as outlined by Williams and Hodgkinson, [9].

2. Experimental Set-up

2.1. One-Point Bend Fracture apparatus

The one-point bend set-up is a modification of the traditional Kolsky bar apparatus [10], where the transmission bar has been removed. The apparatus consists of a single instrumented cylindrical bar of length 300 mm and diameter 3 mm, Fig. 1. In a typical test a striker impacts the leading edge of the incident bar setting up a longitudinal stress wave. This wave propagates down the incident bar towards the specimen and subsequently reflects at the bar/specimen interface. A portion of the wave is transmitted through the interface into the specimen causing fracture. The degree to which the wave is reflected or transmitted depends on the impedance of the bar and specimen material and will be discussed later. It is of the upmost importance that the striker contact with the incident bar be a planar one. This ensures a trapezoidal wave will be generated and avoids any spurious wave reflection at the impact interface. The compressive wave can be well controlled in terms of duration and amplitude by varying the length and velocity of the striker respectively. The striker must remain less then half the incident bar length so to allow complete unloading of the striker before the arrival of the reflected wave from the impact end. The striker and incident bar both must be made of the same material. In a one-point bend configuration the specimen maintains a single point of contact with the loading apparatus. That is, the specimen remains unsupported throughout the test with no supports to restrain the free-body motion of the specimen. In this way the specimen will fracture due to inertia alone.

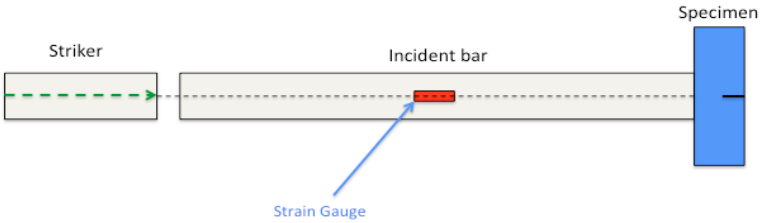

Figure 1. One-Point Bend apparatus

2.2. Material

Tests were carried out using SENB geometries. Due to inherent manufacturing constraints advanced ceramic materials have limitations on available specimen dimensions. Initial testing was carried out on PMMA with specimen span of 18 mm, height of 6 mm and thickness of 3 mm. Testing on the ceramic material was carried out on specimens with a span of 28.5 mm, height 6.25 mm and thickness of 4.76 mm. Future testing will involve specimens whose dimensions are further restricted with a span of 14 mm, height of 5 mm and thickness of 2 mm. The PMMA specimens were notched at 45-degree angle to a depth of 1 mm. Pre-cracks were subsequently introduced using a razor blade. Tests were preformed only on specimens whose pre crack was straight. For brittle materials like ceramics pre cracking is not an option and so samples had a notch root radius of 150 μm for all grades with a notch depth of 1.5 mm. Table 1. shows static fracture toughness values for PMMA and ceramic A and B. The PMMA tests were carried out using the standard three-point bend method, [11]. Static fracture results for the advanced ceramics A and B were taken from a previous study, [12] using a three-blunt notch analytical approach.

Table 1. Static Fracture toughness values

Material	K_{Ic}(MPa$\sqrt{m}$)
PMMA	1.61
Ceramic A	7.70
Ceramic B	2.80

3. Fracture Toughness determination

3.1. Data Reduction

The load applied to the specimen is given below and is based on one-dimensional wave theory, [10]:

$$P(t) = EA_0[\varepsilon_I(t) + \varepsilon_R(t)], \tag{1}$$

where E and A_o are the Young's modulus and cross-sectional area of the bar respectively. The particle velocity at the end of the incident bar is given by:

$$v = C_0[\varepsilon_I(t) - \varepsilon_R(t)], \tag{2}$$

where C_0 is the longitudinal wave velocity of the pressure bar. Integration of the velocity will also yield displacement at the end of the bar.

It is important to note that specimens must be sufficiently brittle so to fully fracture before they loose contact with the incident bar. Once the specimen leaves the end of the bar a free end boundary condition prevails and the above equations are no longer applicable. Up to this time Eq. (1) can be

used to determine the load applied to the specimen up to the point of fracture.

3.2. Fracture time (t_f) Determination

To determine fracture time a small uncalibrated strain gauge was mounted on the specimen close to the crack tip, Fig. 2. The location of the strain gauge is important, as it must be placed within the elastic region but outside the damage zone to yield accurate results [6]. Upon loading, stress within the specimen builds up and the gauge experiences a voltage change. As the crack passes the gauge an unloading wave is generated and a drop of the measured voltage indicates this. The time from the initial voltage rise to the drop off represents the fracture time. Due to the finite size of strain gauges it is difficult to place them exactly at the crack tip. In order to more accurately determine the fracture time a hybrid experimental/numerical approach is undertaken here. Modeling of the fracture specimen using the finite volume method (FVM) was done in OpenFOAM [13,14]. Strain gauge locations on the experimental samples were accurately measured and this data was adopted for the modeling work. Time up to unloading was found to agree well between the two methods. By combining experimental and numerical data increased accuracy of fracture time determination can be ensured.

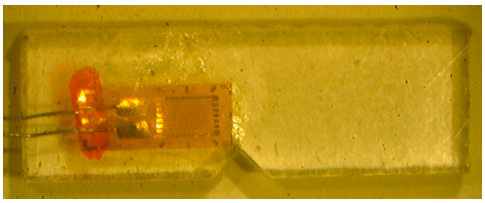

Figure 2. Strain gauge for fracture time detection

3.3. Temporal Stress Intensity Factor Determination

3.3.1. Applied load method

Dynamic fracture toughness (K_{Id}) can be determined as the critical stress intensity factor value at the crack tip at the instant of crack initiation. For Mode I fracture it is approximated as:

$$K_{Id} = K_I(t_f), \tag{3}$$

A closed form solution to predict the SIF from the measured load is applied here [15].

$$K_I(t) = \frac{3SP(t)}{4BW^{3/2}} \frac{\sqrt{\alpha}}{(1-\alpha)^{3/2}(1+3\alpha)} (1.72 + 0.23\alpha + 1.04\alpha^2 - 0.39\alpha^3), \tag{4}$$

where *P(t)* is the applied load to the sample and α is the ratio of crack length to width of the specimen (*a/W*). It has been demonstrated that this equation is valid for different crack to width ratios [8].

3.3.2. Crack tip strain

Another method for determining the SIF evolution experimentally is shown in Eq. (5). This method

relies on the direct measurement of the strain field near the crack tip by means of a strain gauge.

$$K_I(t) = \frac{\varepsilon_y(t) E \sqrt{2\pi r}}{Cos\frac{\theta}{2}\left[1 + Sin\frac{\theta}{2} Sin\frac{3\theta}{2} - \nu(1 - Sin\frac{\theta}{2} Sin\frac{3\theta}{2})\right]}, \quad (5)$$

where r is the radial distance from the crack tip to the strain gauge and θ is the angle from the crack path, [6].

4. Results & Discussion

4.1. PMMA Tests

All tests were performed at ambient temperature. The static fracture toughness has also been determined for comparison. Fig. 3(a) shows a typical incident and reflected strain trace from a fracture test. The striker velocity leaving the muzzle was approximately 8.5 m/s determined using a high-speed camera, which results in a particle velocity of 6 m/s at the load point of the apparatus from Eq. (2). Using Eq. (1) the load applied to the specimen was determined and is illustrated in Fig. 3(b). For this test the value of (a/W) was 0.33 and using Eq. (4) the temporal SIF was found as shown in Fig. 4.

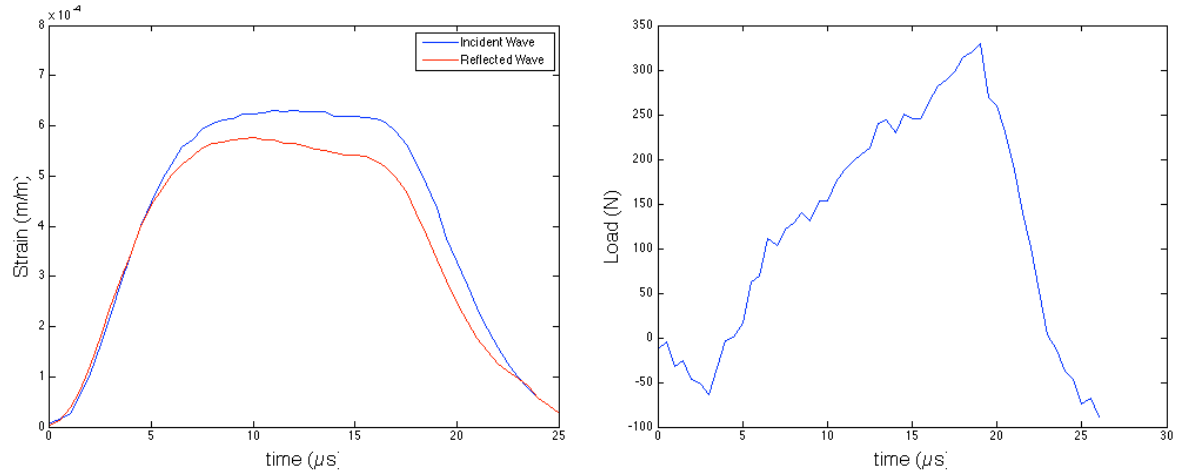

Figure 3(a). Superposition of incident and reflected strain trace, (b) Variation of applied load with time

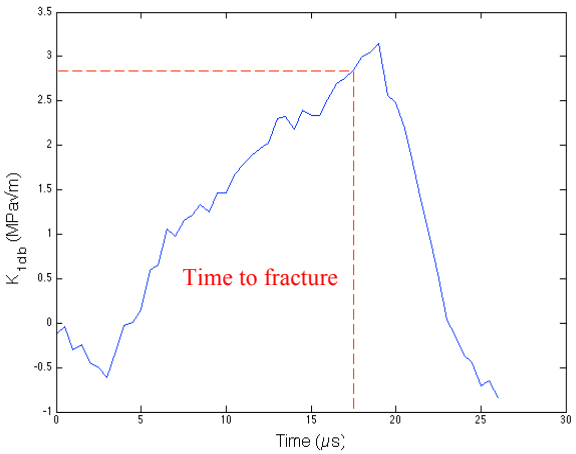

Figure 4. Stress intensity evolution for PMMA at 6m/s

Using both experimental and numerical methods the time to fracture was determined to be 17.5 μs. This yields an apparent dynamic fracture toughness for PMMA of 2.75 MPa√m from the above analysis, Fig. 4.

A number of other tests were carried out at varying loading rates. Fig. 5 shows the stress intensity evolution for a test performed at a velocity of 9.5 m/s. The variation in amplitude of the oscillations between the two tests is as a result of the increased rate of loading.

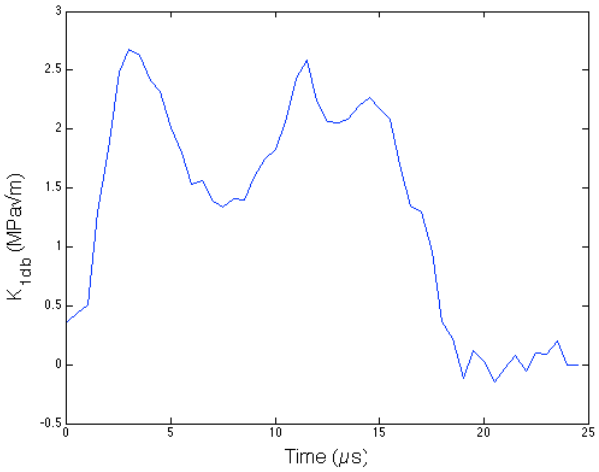

Figure 5. Stress intensity evolution For PMMA at 9.5m/s

Fracture time for the above test was 14.5 μs, which corresponds to an apparent toughness of 2.19 MPa√m. These results agree well with other authors, [5] and show fracture toughness for PMMA increases at dynamic loading rates.

The use of Eq. (5) was shown to greatly underestimate the temporal SIF. For this equation to yield accurate results it is important that the strain measurements be made within the singular zone. The strain gauges used in these tests were 1.5mm in length. Relative to the samples being tested these dimensions are quite large, and while care was taken in their placement, the strain measurements were recorded outside the singular zone therefore leading to inaccurate results. As a result of this the use of strain gauges will be restricted to determining the fracture time for later tests. It should be noted that the use of smaller strain gauges might avoid this problem.

A third method was also tested for comparison. This test procedure uses an impact response curve (IRC) for determination of dynamic fracture toughness, [16,17,18]. This method makes use of the relationship between the dynamic fracture toughness and time to fracture. The IRC is determined once for a specific test condition (impact velocity, specimen material and geometry) using FVM simulation with a contact procedure and subsequently only requires the time to fracture found through experimentation in order to determine the dynamic fracture toughness for successive tests of similar setup.

Fig. 6(a) and (b) show the IRC's determined for an OPB test setup at a particle velocity of 6 m/s using a Young's modulus of 6 GPa and 3 GPa respectively, corresponding to the dynamic and static moduli used by Ivanković and Williams, [19]. In order to determine the IRC for each case the sample was prevented from fracturing. The strain was determined directly at the crack tip in the model within the singular zone, and Eq. (5) was used to calculate the temporal SIF's for these cases. Using the time to fracture determined experimentally from an equivalent test setup the apparent

dynamic fracture toughness is found to be 3.44 MPa√m in the case where the material modulus is taken to be 6 GPa, and 2.84 MPa√m when the modulus is 3 GPa. The model with the higher, dynamic, Young's modulus is shown to overestimate the dynamic fracture toughness when compared to the load-point method presented above. Conversely, when the static Young's modulus of the material (3 GPa) is employed the model predicts an apparent dynamic fracture toughness similar to that of the load-point method, 2.84 MPa√m versus 2.75 MPa√m. This suggests that the static Young's modulus may be a more appropriate measure for this test setup. This point is further reinforced by noting that the quarter period of oscillation (14 µs) of the IRC developed using the dynamic Young's modulus, Fig. 6(a), is less then the experimentally determined fracture time of 17.5 µs, Fig. 4.

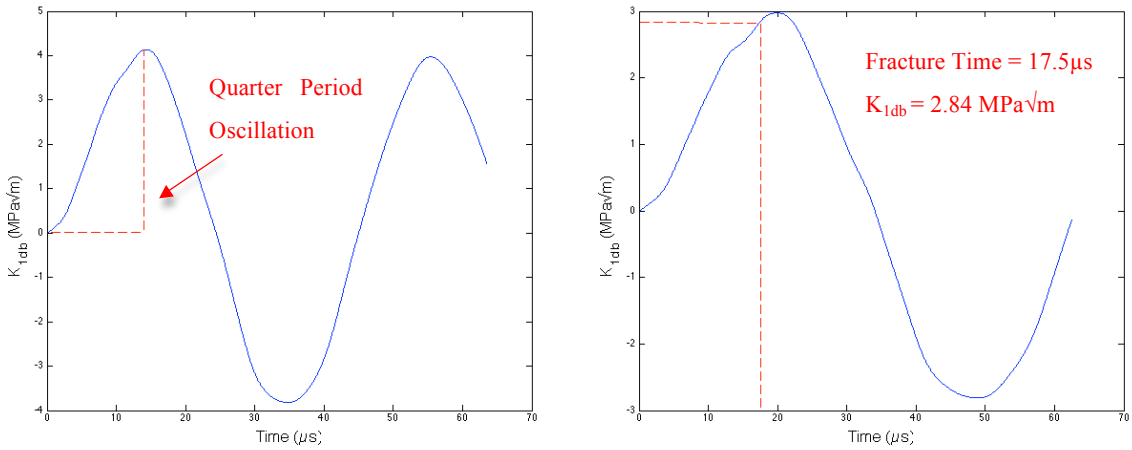

Figure 6(a). Impact Response curve Young's Modulus: 6 GPa, (b) Impact Response curve Young's modulus: 3 GPa

4.2 Advanced Ceramic Tests

A number of tests were carried out on ceramic samples. Due to the inherent difficulty in introducing pre-cracks into hard brittle materials all samples were tested with a blunt notch of 150µm in radius. As a result of this the dynamic fracture toughness values are apparent values. Static fracture toughness values were taken from previous testing [12]. Fig. 7 shows a typical strain trace superimposed on a FVM simulation test with a contact procedure implemented at the incident bar/specimen interface [20]. Very good agreement is observed between experimental and numerical tests. The samples were not instrumented during this round of tests and so only the SIF evolution from the one-dimensional analysis will be calculated. Fig. 8 shows the incident and reflected strain for two tests on samples A and B. The two grades of advanced ceramic vary in both inclusion grain size and second phase material and are denoted A and B. It can be seen from the trace that the degree to which the incident wave is reflected is very similar in both cases. This is to be expected, as at increased rates of loading the values of fracture toughness for both grades of material have been previously shown to be similar [21]. Fig. 9 shows the SIF for both grades of advanced ceramic. The time to fracture for these events was not recorded as mentioned above so a value of fracture toughness at these rates cannot be obtained. It is of interest for future work to instrument the samples using minute strain gauges close to the crack tip as per the PMMA testing. The wave speed velocity in these samples is in the region of 11,000 m/s, resulting in an extremely rapid fracture event. With this in mind future work will also focus on developing the numerical model further to ensure the most accurate determination of fracture time possible.

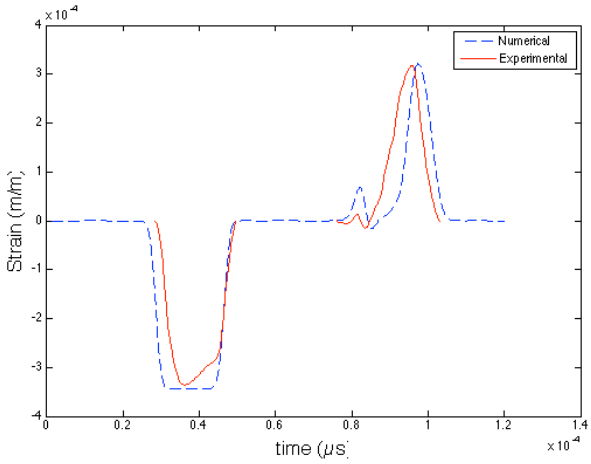

Figure 7. Numerical and experimental incident and reflected wave for ceramic sample

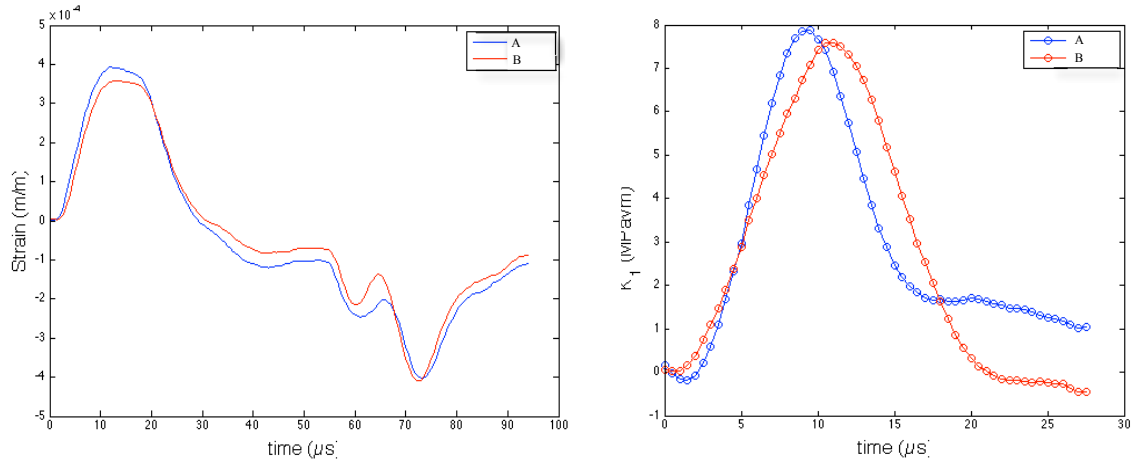

Figure 8(a). Experimental trace from tests on advanced ceramic A & B, (b) SIF evolution for advanced ceramic A & B from Eq. (5)

The difference in the incident and reflected waves in the ceramic tests is much greater than that of the PMMA tests. This is due to the difference in mechanical impedance between the test specimens and the tungsten carbide bar where more of the incident wave was transmitted through the bar/specimen interface. It is desirable to test specimens with similar impedance to that of the bar. In the case of advanced ceramics the impedance difference is low and as a result there is a notable difference between the incident and reflected traces, which allows for the clearer data analysis.

With PMMA its mechanical impedance is much lower then that of the tungsten carbide bars. In view of this fact it is not surprising that the reflected and incident signals are of similar amplitude as very little of the incident wave can be transferred to the specimen for fracture. For relatively low impedance materials it is recommended that a low impedance bar be used as the loading apparatus.

5. Conclusions

A novel experimental method for determining the dynamic fracture toughness of super-hard materials where specimen dimensions are limited was presented. This was achieved using a miniaturized Kolsky bar in one-point fracture. Preliminary tests were undertaken to determine the dynamic fracture toughness of PMMA. It has been shown that at increased loading rates the fracture

toughness of PMMA increases. A comparison of methods to determine SIF evolution was examined. One method using the applied load up to the point of fracture, another method, measuring strain directly on the sample close to the crack tip and a third through the use of an impact response curve. It was shown that strain measurements directly on the sample greatly underestimate the SIF. This is due to the strain measurements being erroneous as they were taken outside the singular zone. The impact response curve yielded apparent dynamic fracture toughness very similar to that of the load-point method. The strain used to calculate the IRC was measured directly on the crack tip in the model, which should lead to a more accurate calculation of SIF even when using static formula. Future testing will focus on detailed experimental work concurrent with numerical analysis to investigate the validity of these methods with emphasis on the use of impact response curves to determine dynamic fracture toughness. No attempt has been made to explain the observed increase in apparent fracture toughness at this stage, although it is in the scope for future testing.

The dynamic SIF evolution of two grades of advanced ceramic was investigated. At high rates of loading the fracture toughness of these grades was shown to decrease from their static values. A numerical model of the one-point bend set up has also been developed and excellent agreement between experimental and numerical results has been achieved. Future work will focus on further development of the model to determine the fracture time, a vital fracture parameter for accurate determination of dynamic fracture toughness.

Acknowledgements

The authors would like to thank Element Six Ltd., Enterprise Ireland and the Irish Research Council for providing financial support for this research.

References

[1] M.G. Charpy, On testing metals by the bending of notched bars. Int. J. Frac. 25 (1984) 287-305.

[2] D.R. Ireland, Critical Review of Instrumental Impact Testing Dynamic Fracture Toughness. The Welding Institute of American Society for Metals, Technical Report (1976) No. 79-55.

[3] W.L. Server, Impact three-point bend testing for notched and precracked specimens. J. Test. Eval., 6.1 (1978) 29-34.

[4] W. Bohme, The influence of stress wave on the dynamic crack tip loading in three- point bend impact. DGM Informationsgesellschaft mbH, Impact Loading and Dynamic Behaviour of Materials, 1 (1988) 305-311.

[5] C. Bacon, J. Farm, J.L. Lataillade, Dynamic fracture toughness determination from load-point displacement. Exp. Mech. 34.3 (1994) 217-223.

[6] G. Weisbrod, D. Rittel, A method for dynamic fracture toughness using short beams. Int. J. Frac., 104.1 (2000) 89-103.

[7] A. Belenky, I. Bar-On, D. Rittel, Static and dynamic fracture of transparent nano-grained alumina. Journal of the Mechanics and Physics of Solids, 58.4 (2010) 484-501.

[8] J. Fengchun, K.S. Vecchio, Hopkinson Bar Loaded Fracture Experimental Technique: A Critical Review of Dynamic Fracture Toughness Tests. Applied Mechanics Review, 62 (2009) 060802.

[9] J.G. Williams and J.M. Hodgkinson, Crack-blunting mechanisms in impact tests on polymers. Proc. R. Soc. Lond. A, 375 (1981) 231-248.

[10] H. Kolsky, An Investigation of the mechanical properties of materials at very high rates of loading. Proc. Phys. Soc Lond, 62.11 (1949) 676.

[11] BSI. Advanced technical ceramics: test methods for determination of fracture toughness of monolithic ceramics. Part 5: single-edge v-notch beam (SEVNB) method. DD CEN 14425-5, British Standards Institution; 2004.

[12] D. Carolan, P. Alveen, A. Ivanković, N. Murphy, Effect of notch root radius on fracture toughness of polycrystalline cubic boron nitride. Eng. Frac. Mech. 78 (2011) 2885-2895.

[13] A. Ivanković and J.G. Williams, The Finite Volume Analysis of Linear Elastic Dynamic Fracture Problems, In *Dynamic Fracture Mechanics*, Chapter **3**, Eds. M. H. Aliabadi, (Computational Mechanics Publications, Southampton), 1995, 101-135.

[14] H. Weller, G. Tabor, H. Jasak, C. Fureby. A tensorial approach to CFD using object oriented techniques. Computers in Physics, 12 (1998) 620– 631 .

[15] I. Villa, J. loya, J. Fernandez-Saez, General expressions for the stress intensity factor of a one-point bend beam, Eng. Frac. Mech., 74.3 (2007) 373-385.

[16] J.F. Kalthoff, S. Winkler, W. Bohme and W. Klemm, Determination of the dynamic fracture toughness K_{1d} in impact by means of response curve. Int. J. Frac. 12 (1980), 277-298.

[17] J.F. Kalthoff, S. Winkler and W. Bohme, A novel procedure for measuring the impact fracture toughness K_{1d} with precracked charpy specimen, Journal de Physique 46 (1985), 363-373.

[18] A. Rager, J.G. Williams and A. Ivanković, Numerical Analysis of the three point bend impact tests for polymers, Int. J. Frac. 135 (2005), 201-217.

[19] A. Ivanković, J.G. Williams, A local modulus analysis of rapid crack propagation in polymers. Int. J. Frac. 64(4) (1993), 251-268.

[20] P. Cardiff, A Karac and A. Ivanković. Development of a finite volume contact solver based on the penalty method. Computational Materials Science (2012).

[21] D. Carolan, A. Ivanković, N. Murphy, A combined experimental-numerical investigation of fracture of Polycrystalline Cubic Boron Nitride. In Press, Accepted Manuscript, Eng. Fract. Mech. http://dx.doi.org/10.1016/j.engfracmech.2012.09.008.